GEOEFFECTIVITY OF CORONAL MASS EJECTIONS

H. E. J. KOSKINEN[1,*] and K. E. J. HUTTUNEN[†]
University of Helsinki, Department of Physical Sciences, P.O. Box 64, FIN-00014 Helsinki, Finland
*(*Author for correspondence: E-mail: Hannu.E.Koskinen@helsinki.fi)*

(Received 18 July 2005; Accepted in final form 9 January 2006)

Abstract. Coronal mass ejections and post-shock streams driven by them are the most efficient drivers of strong magnetospheric activity, magnetic storms. For this reason there is considerable interest in trying to make reliable forecasts for the effects of CMEs as much in advance as possible. To succeed this requires understanding of all aspects related to CMEs, starting from their emergence on the Sun to their propagation to the vicinity of the Earth and to effects within the magnetosphere. In this article we discuss some recent results on the geoeffectivity of different types of CME/shock structures. A particularly intriguing observation is that smoothly rotating magnetic fields within CMEs are most efficient in driving storm activity seen in the inner magnetosphere due to enhanced ring current, whereas the sheath regions between the shock and the ejecta tend to favour high-latitude activity.

Keywords: coronal mass ejections, magnetic clouds, interplanetary shocks, magnetic storms, geomagnetic indices

1. Introduction

The first coronal mass ejection (CME) was detected using the white-light coronagraph on the OSO 7 satellite on December 14, 1971 (Tousey, 1973). The pioneering OSO 7 observations of 20 CMEs were followed by observations on Skylab, P78-1 (Solwind), and SMM in the 1970s and 1980s. The term "coronal mass ejection" describes the observation of a large amount of mass, some $10^{12} - 10^{13}$ kg, being detected in the corona to leave the Sun without implying any physical interpretation, e.g., of its origin.

The CMEs are often but not always found to be closely related to solar flares at a nearby region in the solar atmosphere. The first flare was observed on September 1, 1859 by Carrington (1859) and Hodgson (1859). For solar-terrestrial connections it is interesting that Carrington noted that a magnetic storm commenced about 17 hours and 40 min after the appearance of the flare. According to large number of different records, this event has remained in the top tier of solar-terrestrial events to the present times (Cliver and Svalgaard, 2004). Based on magnetic recording in Bombay, this storm has been claimed to be, by far, the strongest *Dst* storm during the last 150 years (Tsurutani *et al*., 2003). Gradually, this and subsequent coincidences

[1] also at Finnish Meteorological Institute, Space Research Unit
[†] presently at University of California in Berkeley, Space Sciences Laboratory

Space Science Reviews (2006) 124: 169–181
DOI: 10.1007/s11214-006-9103-0

of solar flares and magnetic storms led to the concept that the solar flares indeed were the sources of strong magnetic activity on Earth (Hale, 1931).

The discovery of CMEs started slowly to change this picture. An increasing fraction of solar-terrestrial scientists began to appreciate the fundamental role of the CMEs and the interplanetary shocks as the drivers of major non-recurrent magnetospheric storms, but a large fraction of the magnetospheric and ionospheric community continued to refer to flares as the primary cause of magnetic storms. This continued until the 1990s, as noted by Gosling (1993) in his landmark article "The Solar Flare Myth".

A critical turning point was reached in January 1997. A group of scientists were following real-time data from SOHO instruments when they observed a bright halo around the occulting disk of the LASCO coronagraph on January 6, 1997, which they interpreted as an earthward-directed CME. They alerted the space weather service at NOAA of a possibly approaching storm, but as there were no other indications of an approaching storm, the alert was ignored. The interplanetary shock at 1 AU was observed by WIND on January 10 at 0010 UT. Thus the CME was rather slow and caused a medium-size storm in the magnetosphere ($Dst_{\min} = -78$ nT and $Kp_{\max} = 6$). What made this event so important was that it led to an accumulation of a large flux of relativistic electrons in the outer radiation belt, which was suggested to have been the cause of the loss of the geostationary telecommunication satellite Telstar 401 on January 11. Next day, this was in the news world wide, and the importance of CMEs finally penetrated throughout the magnetospheric research community. The event was discussed in a series of papers in a special issue of *Geophysical Research Letters* (vol 25(14), 1998).

After leaving the corona CMEs are called interplanetary CMEs (ICMEs) or ejecta. Signatures of ejecta have been discussed and summarized extensively, e.g., by Zwickl *et al*. (1983), Gosling (1990) and Neugebauer and Goldstein (1997). Magnetic field and solar wind plasma signatures of ICMEs include enhanced magnetic field strength and low variation of magnetic field, unusually low proton temperatures and bidirectional flux of suprathermal electrons. Plasma compositional anomalies, such as increased helium to proton ratio and enhancements of minor ions, also indicate the presence of an ICME. The above mentioned studies, however, point out that there is no unambiguous way to identify an ICME. Most ICMEs exhibit only some of the features and different signatures do not necessarily coincide spatially.

Magnetic clouds (Burlaga *et al*., 1981) are an important subset of ejecta, in particular for our study, as they contain the strongest magnetic fields in the solar wind. Their signatures are the smooth rotation of the magnetic field direction over a large angle, large magnetic field intensity and low proton beta. The fraction of magnetic clouds of all ejecta varies with the phase of the solar cycle. During the ascending phase of solar cycle 23 almost all ejecta around solar minimum were magnetic clouds, whereas near maximum the fraction decreased below 20% (Richardson and Cane, 2003).

An ICME moving at supersonic (super-Alfvénic) speed with respect to the background solar wind produces a shock front ahead of it. The sheath regions between the shock and the ejecta form another class of highly geoeffective solar wind structures. The role of the shocks in Sun-Earth connections is twofold. First, shocks are efficient accelerators of protons and helium nuclei. The enhanced levels of energetic ions caused by both solar flares and CME-driven shocks provide hazardous environment not only near Earth but also elsewhere in the solar system. Second, from the magnetospheric viewpoint the most important feature of the ICMEs and shocks is their capability of shaking the entire magnetosphere through variable plasma pressure and by the dynamics related primarily to the direction of the interplanetary magnetic field (IMF). A fast plasma cloud can increase the dynamic plasma pressure by a large factor pushing the dayside magnetopause from its nominal distance of about $10R_E$ inside the geostationary orbit at $6.6R_E$. This can already be serious for spacecraft that are designed to remain inside the magnetosphere and, e.g., use the geomagnetic field for attitude control. However, as we will discuss below, the direction of the IMF is the most decisive factor.

2. Propagation from the Sun to the Earth

Even a relatively complete knowledge of CME properties in the corona is only the first step toward a reliable prediction of its geoeffectivity. We have very little observations on details of any specific ICME after it has left a coronagraph's field-of-view. An example of this is the disappearance of the bright kernel often seen in the coronagraph images. The kernel is likely cool matter from the erupted prominence. However, this structure is difficult to identify in plasma observations at 1 AU. A useful signature of prominence matter is high He^{+}/He^{++} ratio (Schwenn *et al.*, 1980; Zwickl *et al.*, 1983; Skoug *et al.*, 1999). However, such events are rare. According to Lynch *et al.* (2003) from the entire time period (before mid-2002) during which reliable composition data were available from WIND and ACE less than 10 events were observed with unusually low charge state ratios. A specific feature of the January 1997 event was very dense cool plasma near the trailing edge of the ICME, which may have been a remnant of the filament matter (Burlaga *et al.*, 1998; Webb *et al.*, 2000).

Observation of the evolution of an ICME is a formidable problem (Gopalswamy, 2006). With *in-situ* satellite observations we get data along a single line through a moving ICME. With more than one spacecraft the situation is improved, but owing to the very large size of the ICMEs the measurement points need to be well separated from each other. Radio wave observations in the megahertz range (e.g., WAVES onboard WIND observing at frequencies below 14 MHz) provide a global means of following the propagation of some CME-driven shocks into the solar wind (e.g., Reiner and Kaiser, 1999; Gopalswamy *et al.*, 2001). While this method gives valuable information of the early motion of some shocks, it has not yet matured to

the level where it could be used for predicting the geoeffectivity of the shock and the CME.

3. Storms Seen in Geomagnetic Indices

The strength of magnetospheric perturbations is usually described using some of the several magnetic activity indices (Mayaud, 1980). Different indices emphasize different features of magnetic activity and one has to be careful when considering which aspects one wants to highlight when selecting an index to organize the data. Here we use two of the most popular indices in this context: *Dst* and *Kp*.

The *Dst*-index is a weighted average of the deviation from the quiet level of the horizontal (H) magnetic field component measured at four low-latitude stations around the world. The westward ring current flowing around the Earth at the distance of about 3–4 R_E is the main source of the *Dst*-index. During a magnetospheric storm the ring current is enhanced, which causes a negative deviation in H. Consequently, the more negative the *Dst*-index is, the stronger the storm is said to be. In the present discussion we set the threshold between weak and moderate storms to -50 nT in *Dst*, moderate storms range from -50 to -100 nT. Storms stronger than -100 nT are called intense and stronger than -200 nT big. The *Dst*-index is calculated once an hour. A similar 1-minute index derived from a partly different set of six low-latitude stations (SYM–H) is also in use.

However, the magnetometers used to calculate *Dst* are also influenced by current systems other than the ring current. High solar wind pressure pushes the magnetopause closer to the Earth both increasing the magnetopause currents and moving them closer to the observation point. Thus a pressure pulse impinging on the dayside magnetopause causes a positive deviation in the H-component. If the solar wind parameters are known, the effect can be cleaned away from the *Dst*-index (so-called pressure corrected *Dst*-index). More difficult is to estimate the effect of the dawn-to-dusk directed magnetotail current. During strong activity the tail current enhances significantly and the current sheet moves closer to the Earth, enhancing the *Dst*-index. It is a controversial issue in magnetospheric physics how to handle this effect

Another widely used index is the planetary K-index *Kp*. Each magnetic observatory has its own perturbation index K, which indicates the range of the maximum perturbation during a 3-hour interval. *Kp* is an average of the K-indices from 13 mid-latitude stations. *Kp* is expressed in a scale of one-thirds: $0, 0+, 1-, 1, \ldots, 8+, 9-, 9$. As *Kp* is based on mid-latitude observations, it is more more sensitive to high-latitude auroral currents than is the *Dst*-index.

Figure 1 illustrates the evolution of the storm strength in a case where two CMEs were released successively from the same region on the Sun. The CMEs were observed as halos by LASCO on March 28, 2001, at 1300 UT and on March 29 at 1030 UT. The times refer to the first observation of the CME edge in the LASCO

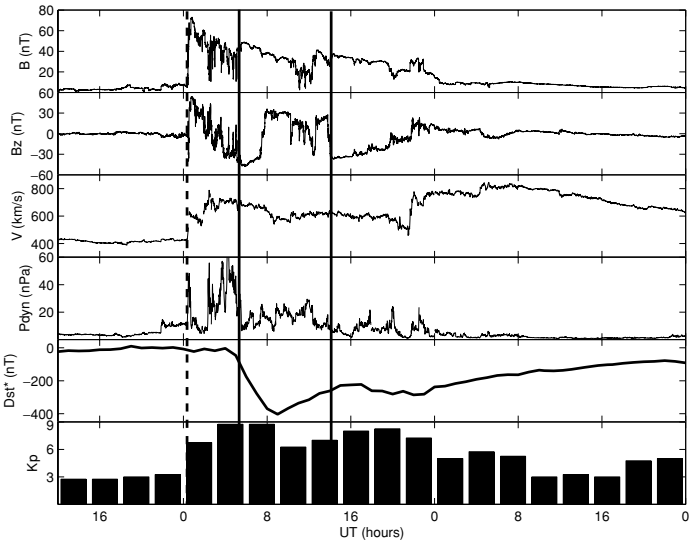

Figure 1. A double-peaked storm driven by two consecutive ICMEs. Upstream solar wind data from ACE are given in the top four panels: IMF intensity, IMF north-south component, plasma velocity, and dynamical pressure. The fifth panel gives the pressure corrected *Dst*-index and the lowermost panel the *Kp*-index. The shock is indicated by the dashed line and the arrivals of the magnetic clouds by the solid lines. The data interval is from 30 March, 2001, 12 UT to 1 April, 2001, 24 UT.

C2 coronagraph. A strong (X1.7) flare was associated with the latter (March 29 at 1015 UT). In such cases the latter ICME often has a higher velocity than the former and catches it on the way out to 1 AU. In this case the initial speed difference was estimated to be 350 km/s and the time interval between the arrival times at 1 AU had reduced to about 8.5 h.

In Figure 1 the shock (dashed line) preceding the first CME as well as the beginning of the smooth magnetic cloud structures (solid lines) are well visible. The end of the first CMEs is more unclear. Note that the total magnetic field remains at a relatively high level. Thus the Alfvén speed is large and no clear shock structure before the second magnetic cloud can be identified.

These ICMEs led to the third biggest storm of cycle 23: $Kp_{\max} = 9-$ and $Dst_{\min} = -387$ nT. This was an example of a double-peaked storm. More typically the first *Dst*-minimum of a double-peaked storm is due to the sheath region and the second to the ejecta (Kamide *et al.*, 1998).

This event illustrates that there is no one-to-one correlation between the storm strengths given by *Kp* and *Dst*. The *Kp*-activity reached storm level soon after the interplanetary shock had hit the magnetopause. Note that the *Dst*-index in Figure 1 is given pressure-corrected, which has removed the shock effect on its trace. A strong *Kp*-storm was in progress while the flow and magnetic field were fluctuating in the sheath region for several hours before the main phase of the

Dst-storm commenced. This happened slightly before the arrival of the magnetic cloud, which is characterized by the smooth evolution of the IMF Z-component. After the first cloud the *Dst*-index started to recover slowly as did the *Kp*-index. While the *Dst*-storm was recovering, the solar wind parameters became again more variable in the region between the two magnetic clouds and the *Kp*-index started to enhance again, whereas the second minimum in *Dst* was reached only after the arrival of the second cloud.

In the following we define a magnetic storm as sheath-associated if 85% of the *Dst* minimum occurred while the dayside magnetosphere was embedded in the CME sheath region. For a magnetic cloud-associated storm we require that during a magnetic cloud passing the magnetosphere *Dst* reached the intense storm level of −100 nT and that for two-step storm developments the time difference between two consecutive *Dst* minima was at least 3 hours. Note that the impact of a pre-existing ring current population is not particularly important in creating a stronger intensification later in a storm (Kozyra *et al*., 2002).

Huttunen *et al*. (2002) investigated the difference of the *Kp*- and *Dst*-responses to different solar wind drivers during 1996–1999. They found that the fast post-shock streams and sheath regions had a relatively stronger effect on the *Kp*-index, whereas the effects of ejecta favoured the *Dst*-index. This tendency was emphasized further in by Huttunen and Koskinen (2004) who compared the evolution of several magnetic indices (*Dst*, SYM–H, ASY–H, AE, and *Kp*) during magnetic cloud and sheath region storms. The difference in the response of magnetic indices is most clear when sheath regions and magnetic clouds, i.e., not all ejecta, are compared because solar wind dynamic pressure and the magnetic field direction behave most differently within these structures.

In Figure 2 we have collected the maximum *Kp* and minimum *Dst* indices of all intense storms ($Kp_{\max} \geq 7-$ or $Dst_{\min} < -100$ nT) during 1997–2003 that we could associate clearly with a sheath region or with a magnetic cloud. From these data it is evident that most of the large *Kp* storms were sheath storms as well as all large *Kp* – smaller *Dst* events, whereas large *Dst* – smaller *Kp* events were mostly associated with magnetic clouds.

We do not yet have a complete explanation what causes this difference in the index response. Our hypothesis is that it is related to the fact that *Kp* is more sensitive to auroral zone current systems than *Dst*. This is supported by our investigation of the storm response in the SYM–H and auroral electrojet indices (Huttunen and Koskinen, 2004), where we illustrated using four sample events that the high *Kp*-activity really was due to strongly enhanced auroral activity and not just an artifact produced by the procedure to derive the *Kp* index.

This leads us to propose the following scenario: The irregularities in the sheath region cause perturbations in the magnetopause low-latitude boundary layer, which enhance the Region 1 current system that couples to the auroral current systems in the ionosphere. Consequently the auroral activity is enhanced, which shows up more strongly in *Kp* than in *Dst*. On the other hand, the smooth rotation of the magnetic

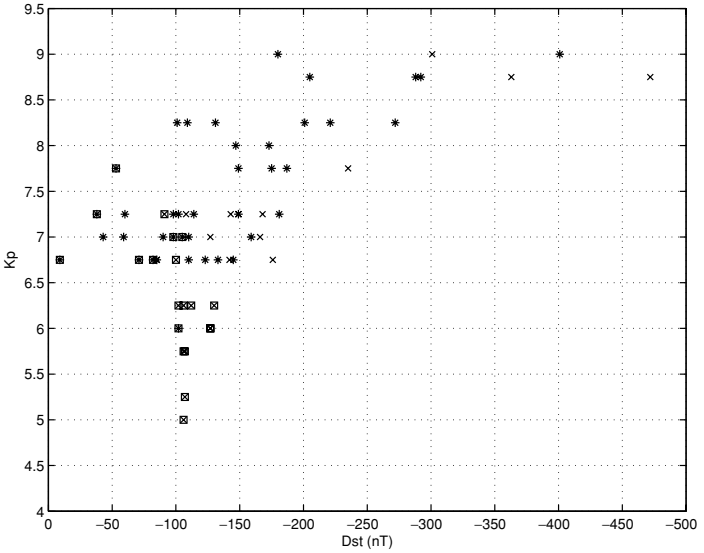

Figure 2. *Kp*- and *Dst*-indices for all intense storms ($Kp_{\max} \geq 7-$ or $Dst_{\min} < -100$ nT) during 1997–2003 that we could associate clearly with a sheath region (asterisks) or with a magnetic cloud (crosses). The rectangles identify storms that did not fulfil the intense storm condition: $Kp \geq 6-$ over three 3-h intervals, by Gosling *et al*. (1991).

cloud field does not cause the same effect on the high-latitude current systems but strengthens the large-scale magnetospheric convection which leads to ring current build-up and enhanced *Dst*-effect. Note that this is not an either-or question, as we deal with relatively large storms where both ring current and auroral current systems are activated. The large-scale convection also enhances the auroral currents. In fact, we have not encountered *Dst*-storms without significant high-latitude activity but there are examples of *Kp*-storms with very weak *Dst*-response. Several examples of this are seen in Figure 2.

Gosling and McComas (1987) suggested that the draping of the magnetic field lines around the ejecta could cause prolonged periods of southward IMF, which might be an important factor in simulating geomagnetic activity. The importance of the sheath regions as efficient storm drivers was demonstrated by Tsurutani *et al*. (1988), but their significance not been widely appreciated before the more extensive analyses of *in situ* observations from solar cycle 23 (Wu and Lepping, 2002; Huttunen *et al*., 2002).

Huttunen and Koskinen (2004) showed that 45% of 53 intense ($Dst < -100$ nT) storms were caused by a sheath region (i.e., the sheath caused at least 85% of the *Dst* depression). When the threshold was changed to $Dst < -150$ nT, already 60% of the remaining storms were sheath-driven (Figure 3). The number of events is too small to make statistical conclusions of this feature, but the study clearly shows the importance of sheath regions as storm drivers.

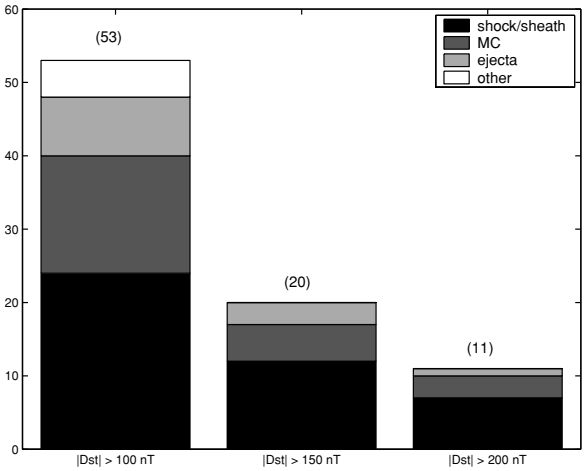

Figure 3. Drivers of intense *Dst*-storms (from Huttunen and Koskinen, 2004).

4. What Determines the Geoeffectivity of ICMEs

The concept of reconnection was introduced to magnetospheric physics by Dungey (1961) who proposed that the magnetospheric convection was driven by magnetic reconnection on the dayside magnetopause. A few years later (Fairfield and Cahill, 1966) demonstrated a statistical correlation between the direction of the IMF and the intermittent magnetospheric activations observed best in the auroral zone, the substorms.

In reconnection theory the reconnection rate is expressed in terms of the reconnection electric field, which in this case is $E = vB_s$, where v is the solar wind speed and B_s the southward component of the IMF. A fast ICME can enhance both factors. The velocities of the shock, the ICME and the post-shock streams can easily be more than twice the background solar wind speed. The IMF in the sheath region between the shock and the ejecta is strongly compressed. If the IMF ahead of a fast ICME already has a southward component, the shock increases it typically by a factor of 3–4. This way the sheath region can drive a storm even if the ICME itself does not hit the magnetosphere. The southward IMF component may be further amplified by draping of the magnetic field around the ICME (Gosling and McComas, 1987), which can lead to a southward IMF component even in cases where the pre-existing IMF is slightly northward. This mechanism works also when the ICME is too slow for shock formation.

Finally, the strongest long-lasting southward magnetic fields in the solar wind are found within magnetic clouds that according to their definition exhibit flux-rope structure determined by the eruptive magnetic structure on the Sun. For example, on November 20, 2003, the north-south magnetic field component of an ICME reached -53 nT, which is an order of magnitude more than typical IMF at 1 AU.

The south component of the IMF is the most critical parameter to determine the geoeffectivity of an ICME. High speed and pressure also perturb the magnetosphere, but they do not cause large-scale storm development if the IMF does not turn to the south. Depending on the background solar wind conditions and on the magnetic structure of the ICME a large number of alternative storm evolutions can take place (Tsurutani *et al*., 1988; Wu and Lepping, 2002; Zhang *et al*., 2004; Huttunen *et al*., 2005).

If the shocked IMF has northward orientation, the sheath region is not yet geoeffective and the storm main phase will not begin until a southward IMF arrives with the magnetic cloud. On the other hand, if the background IMF has even a small southward component, it is enhanced in the sheath and in case of strong enough southward IMF the sheath can drive a strong storm alone.

In cases of well-defined flux-ropes the orientation of the flux-rope axis and the direction the magnetic field is wound varies (Bothmer and Schwenn, 1994). If the inclination of the flux-rope from the ecliptic plane is small, the magnetic structure is bipolar and can arrive with northward (NS) or southward (SN) magnetic field ahead, which obviously give different evolution for the storm. For example, if a southward sheath field is followed by an NS-type cloud with sufficiently strong and long-lasting southward IMF, a double-peaked *Dst*-storm or even two separate storms may follow. Double- or multiple-peaked storms may also take place if several CMEs have been released toward the Earth from the same active region on the Sun.

A flux-rope can also have a large inclination with respect to the ecliptic. In such cases the IMF can have a unipolar orientation either northward (N) or southward (S) throughout the passage of the flux-rope. In the northward case the ICME will most likely pass the Earth with only minor perturbations, whereas the continuously southward case may lead to a really strong storm.

Figure 4 shows the results of an analysis of 73 magnetic cloud events identified in Wind and ACE observations during solar cycle 23 (Huttunen *et al*., 2005). Unipolar southward clouds always caused at least a medium-size storm ($Dst < -50$ nT), whereas in northward cases only sheath regions caused storms. Note that about one third of the bipolar, either NS or SN, clouds did not lead to a medium-size or larger storm, which is a problem for forecasters. These results are consistent with those by Wu and Lepping (2002) based on 34 magnetic clouds in WIND data during 1995–1998 and by Zhang *et al*. (2004) based on 104 magnetic clouds in ACE data from January 1998 to April 2002. The slight differences in relative percentages likely are due to different selection criteria for a magnetic cloud. Note that Zhang *et al*. (2004) included weak storms (-30 nT $> Dst > -50$ nT) in their study.

5. The Strongest Storms of Cycle 23

Statistically the Earth's magnetic environment is most active somewhat before or after the sunspot maximum. In October 2003, when the overall solar activity was

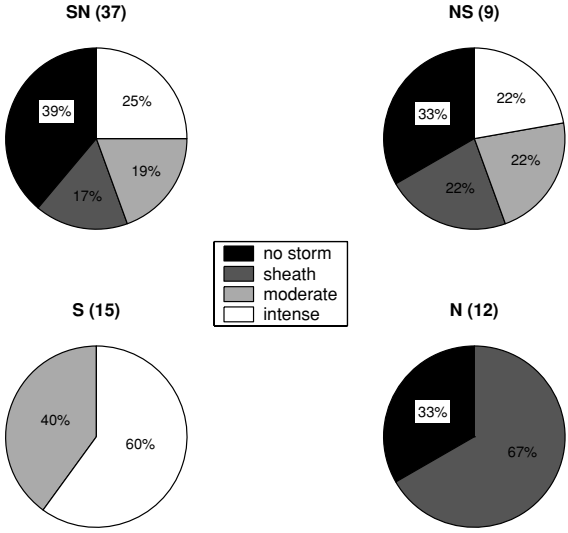

Figure 4. The effect of the flux rope type to the geoeffectivity. Numbers in the parenthesis indicate the total number of magnetic clouds in each category. Color codes are: black – no medium-size or larger storms ($Dst > -50$ nT), dark gray – sheath region storm, light gray – moderate magnetic cloud storm, white – intense magnetic cloud storm (From Huttunen *et al*., 2005).

descending, a period of very strong activity took place (the so-called Halloween events). Several big flares, the largest one reaching X17 on October 28 with an associated halo CME, led to very disturbed conditions. The maximum *Kp* was 9 and the minimum of the (preliminary) *Dst*-index was –401 nT.

The energetic particle fluxes were so intense that several spacecraft, including SOHO, were switched to the safe mode in order to protect sensitive electronics. Large number of satellite anomalies were reported and the effects reached all the way to the ground. For example, in the Gothenburg region in Sweden the electric distribution system went down and anomalously strong geomagnetically induced current was observed in the Finnish natural gas pipeline system.

The source region on the Sun remained active and erupted again one week later on November 4, 2003, now on the western limb. This was the strongest recorded X-ray flare (X28) so far. The consequences of this event did not reach the Earth and we will never know how severe the following storm would have been.

After these magnificent events the strongest *Dst* storm of cycle 23 came as a little surprise. A large filament disappeared from the solar disk between 0740 and 0800 UT on November 18, 2003. At the same time two medium size (M-class) flares were detected at 0752 and 0831 UT and two fast CMEs were identified in LASCO images (0806 UT, 1223 km/s; 0850 UT, 1660 km/s).

However, there was no indication that a particularly strong event would be expected until the shock arrived at 1 AU on November 20, 2003, at 0727 UT (Figure 5). The shock was followed by a particularly strong magnetic cloud. The

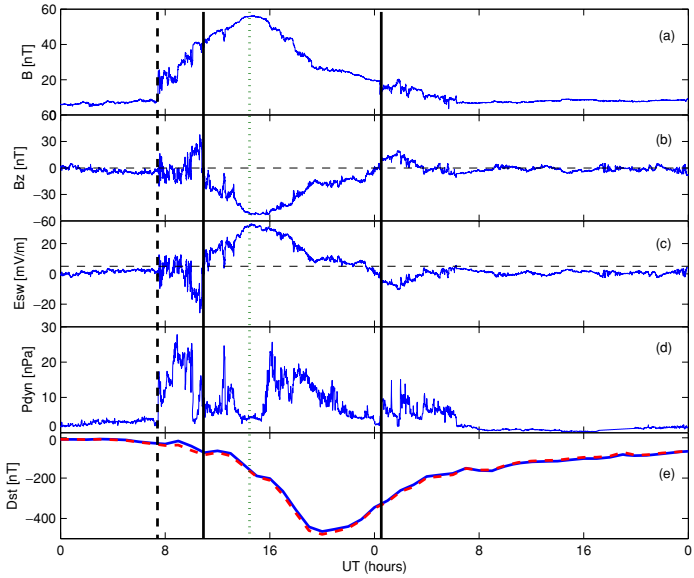

Figure 5. Solar wind parameters from ACE and the *Dst*-response during the November 20 storm. The panels from top to bottom are: IMF intensity, IMF north-south component, east-west component of the solar wind electric field ($E = -v_x B_z$), dynamic pressure and the *Dst* index. In the *Dst* panel also the pressure corrected *Dst* is given by the dashed line. The vertical solid lines indicate the time ACE was within the magnetic cloud (From Huttunen *et al.*, 2005).

maximum magnetic field intensity was about 60 nT and the southward component reached 53 nT. In addition the plasma density of the cloud was large. The resulting storm intensity was 9– in the *Kp* index (interval 15–21 UT) and $Dst_{\min} = -472$ nT (at 20 UT; preliminary value).

The maximum *Kp* or minimum *Dst* are not the only ways of categorizing storms. For practical space weather purposes also the duration of the storm is of great interest. In this sense the Halloween storm was certainly more severe than the November 20 event. During the Halloween storm the *Kp* index was 9 during 9 hours, 9– during another 9 hours and remained above 5– for 60 hours (2.5 days), whereas the November 20 storm was at its highest *Kp* level only 6 hours.

6. Discussion and Conclusions

The different response of different magnetospheric activity indices to sheath regions and ejecta as storm drivers (Huttunen *et al.*, 2002; Huttunen and Koskinen, 2004) is quite interesting. We interpret it to be due to different response of the auroral and ring current systems to the different drivers, as the drivers are structurally quite different. Most notably the magnetic field of a magnetic cloud has a smooth structure of a flux-rope whereas the large-scale field of the sheath is quite unsteady, but it is unclear

how these differences are transferred to the magnetosphere. There have been some attempts to associate upstream solar wind fluctuations with the magnetospheric activity but with rather modest success (e.g., Borovsky and Funsten, 1998).

For practical forecasting purposes we need to learn more what determines the CME parameters on the Sun and whether or not it will be possible to recognize them in advance. To reliably predict the magnetic structure of earthward directed ICMEs from solar observations has shown to be a quite challenging task (e.g., McAllister *et al*., 2001). Also the evolution and propagation of the ICMEs must be better understood. The present propagation time estimates based on halo CME data yield large errors in estimated shock arrival times. Further timing uncertainty is due to the fact that in some cases the storm commences already soon after the shock arrival but in other it does not happen until the rear end of the magnetic cloud reaches the magnetosphere (northward B in the sheath and a NS-type magnetic cloud).

The upcoming STEREO mission of NASA will be very important. The CMEs will be possible to follow visually longer distances from the Sun than earlier and the stereoscopic view will give much better data of the three-dimensional structure of individual CMEs. It is also advantageous to be able to see the Earthward directed CMEs from an angle, as the intensity of halo observations is weaker causing large uncertainties to the initial velocity determination. The *in situ* observations on both sides of the Earth will lead to much better information of the global structure of ICMEs hitting the Earth. On the other hand, when the two STEREO spacecraft will have moved too far from the Earth, they will no longer encounter the solar wind affecting the Earth's magnetosphere. Thus it will be of utmost importance to maintain also the *in situ* upstream observations.

Acknowledgements

We are grateful to R. Schwenn and V. Bothmer for collaboration in our CME studies on LASCO data. The support from the solar-terrestrial physics and space weather groups at the Finnish Meteorological Institute is warmly acknowledged. Much of the results presented here were obtained through the SWAP project supported by the Academy of Finland within the space research programme Antares. The data plots in this review are based on data available in the CDAWeb (Wind and ACE) and at the WDC C2 in Kyoto. The organizers and participants of the very inspiring ISSI workshop are also gratefully acknowledged.

References

Borovsky, J. E., and Funsten, H. O.: 2003, *J. Geophys. Res.* **108**(A6), 1246, doi: 10.1029/2002JA009601.

Bothmer, V., and Schwenn, R.: 1994, *Space Sci. Rev.* **70**, 215.

Burlaga, L., Fitzenreiter, R., Lepping, R., Ogilvie, K., Szabo, A., Lazarus, A., *et al*.: 1998, *J. Geophys. Res.* **103**(A1), 277.

Burlaga, L., Sittler, E., Mariani, F., and Schwenn, R.: 1981, *J. Geophys. Res.* **86**, 6673.
Carrington, R. C.: 1859, *Mon. Not. R. Astron. Soc.* **XX**, 13.
Cliver, E. W., and Svalgaard, L.: 2004, *Solar Phys.* **224**, 407.
Dungey, J. W.: 1961, *Phys. Rev. Lett.* **6**, 47.
Fairfield, D. H., and Cahill Jr., L. J.: 1966, *J. Geophys. Res.* **71**, 155.
Gopalswamy, N., Yashiro, S., Kaiser, M. L., Howard, R. A., and Bougeret, J.-L.: 2001, *J. Geophys. Res.* **106**(A12), 29219.
Gopalswamy, N.: 2006, *Space Sci. Rev.*, this volume, doi: 10.1007/s11214-006-9102-1.
Gosling, J. T.: 1990, in C. T. Russell, E. R. Priest, and L. C. Lee, (eds.), *Physics of Magnetic Flux Ropes*. Geophys. Monogr. **58**, 3518.
Gosling, J. T.: 1993, *J. Geophys. Res.* **98**, 18937.
Gosling, J. T., and McComas, D. J.: 1987, *Geophys. Res. Lett.* **14**, 335.
Gosling, J. T., McComas, D. J., Phillips, J. L., and Bame, S. J.: 1991, *J. Geophys. Res.* **96**, 7831.
Hale, G. E.: 1931, *Astrophys. J.* **73**, 379.
Hodgson, R.: 1859, *Mon. Not. R. Astron. Soc.* **XX**, 15.
Huttunen, K. E. J., and Koskinen, H. E. J.: 2004, *Annales Geophysicae* **22**, 1729.
Huttunen, K. E. J., Koskinen, H. E. J., and Schwenn, R.: 2002, *J. Geophys. Res.* **107**(A7), doi: 10.1029/2001JA900171.
Huttunen, K. E. J., Schwenn, R., Bothmer, V., and Koskinen, H. E. J.: 2005, *Annales Geophysicae* **23**, 625.
Kamide, Y., Baumjohann, W., Gonzalez, W., Tsurutani, B. T., Daglis, I. A., Brekke, A., *et al.*: 1998, *J. Geophys. Res.* **103**, 6917.
Kozyra, J. U., Liemohn, M. W., Clauer, C. R., Ridley, A. J., Thomsen, M. F., Borovsky, J. E., *et al.*: 2002, *J. Geophys. Res.* **107**(A8), doi: 10.1029/2001JA000023.
Lynch, B. J., Zurbuchen, T. H., Fisk, L. A., and Antiochos, S. K.: 2003, *J. Geophys. Res.* **108**(A6), doi: 10.1029/2002JA0009591.
Mayaud, P. N.: 1980, *Geophys. Monogr, 22*, AGU, Washington, D.C.
McAllister, A. H., Martin, S. F., Crooker, N. U., Lepping, R. P., and Fitzenreiter, R. J.: 2001, *J. Geophys. Res.* **106**, 29185.
Neugebauer, M., and Goldstein, R.: 1997, in N. Crooker, J. A. Joselyn, and J. Feynman, (eds.), *Coronal Mass Ejections*, Geophys. Monogr. **99**, 245.
Reiner, M. J., and Kaiser, M. L.: 1999, *J. Geophys. Res.* **104**(A8), 16979.
Richardson, I. G., and Cane, H. V.: 2003, *J. Geophys. Res.* **108**(A4), 1356, doi: 10.1029/2002JA009817.
Skoug, R. M., Bame, S. J., Feldman, W. C., Gosling, J. T., McComas, D. J., Steindber, J. T., *et al.*: 1999, *Geophys. Res. Lett.* **26**(2), 161.
Schwenn, R., Rosenbauer, H., and Mühlhäuser, K.-H.: 1980, *Geophys. Res. Lett.* **7**, 201.
Tousey, R.: 1973, *Space Res.* **XIII**, 713.
Tsurutani, B. T., Gonzalez, W. D., Tang, F., Akasofu, S. I., and Smith, E. J.: 1988, *J. Geophys. Res.* **93**, 8519.
Tsurutani, B. T., Gonzalez, W. D., Lakhina, G. S., and Alex, S.: 2003, *J. Geophys. Res.* **108**(A7), 1268, doi: 10.1029/2002JA009504.
Webb, D. F., Cliver, E. W., Crooker, N. U., St. Cyr, O. C., and Thompson, B. J.: 2000, *J. Geophys. Res.* **105**, 7491.
Wu, C. C., and Lepping, R. P.: 2002, *J. Geophys. Res.* **107**(A10), 1314, doi: 10.1029/2001JA000161.
Zhang, J., Liemohn, M. W., Kozyra, J. U., Lynch, B. J., and Zurbuchen, T. H.: 2004, *J. Geophys. Res.* **109**, A09101, doi: 10.1029/2004JA010410.
Zwickl, R. D., Asbridge, J. R., Bame, S. J., Feldman, W. C., Gosling, J. T., and Smith, E. J.: 1983, in M. Neugebauer, (ed.), *Solar Wind Five*, NASA Conf. Publ., 2280, 711.